

NON-ASYMPTOTIC PERFORMANCE ANALYSIS OF DOA ESTIMATION BASED ON REAL-VALUED ROOT-MUSIC

Junyang Liu¹, Weicheng Zhao², Qingping Wang^{3,†}, Xiangtian Meng⁴, Maria Greco⁵, Fulvio Gini⁵

¹ Department of Computing, The Hong Kong Polytechnic University, Hong Kong, China

² School of Electronics and Information Engineering, Harbin Institute of Technology, Harbin, China

³ State Key Laboratory of CEMEE, National University of Defence Technology, Changsha, China

⁴ School of Information Science and Engineering, Harbin Institute of Technology, Weihai, China

⁵ Department of Information Engineering, University of Pisa, Pisa, Italy

ABSTRACT

This paper presents a systematic theoretical performance analysis of the Real-Valued root-MUSIC (RV-root-MUSIC) algorithm under non-asymptotic conditions. A well-known limitation of RV-root-MUSIC is the estimation ambiguity caused by mirror roots, which are typically suppressed using conventional beamforming (CBF). By leveraging the equivalent subspace constructed through the conjugate extension method and exploiting the equivalence of perturbations for true and mirror roots, this work provides a comprehensive study of three key aspects: noise subspace perturbation, true-root perturbation, and mirror-root perturbation. A statistical model is established, and generalized perturbation expressions are derived. Monte Carlo simulations confirm the correctness and effectiveness of the theoretical results. The analysis provides a rigorous foundation for parameter optimization in Direction-of-Arrival (DOA) estimation, with applications in radar, wireless communications, and intelligent sensing.

Index Terms— RV-root-MUSIC, DOA estimation, non-asymptotic performance analysis, perturbation-theoretic expressions

1. INTRODUCTION

Direction-of-Arrival (DOA) estimation is a fundamental non-linear parameter estimation problem. Accurate parameter acquisition is essential for reliable target perception in diverse applications, including radar detection, wireless communications, sonar localization, and medical imaging [1–7]. However, unavoidable noise contamination during signal transmission and reception introduces estimation errors, making accuracy a key criterion for evaluating algorithmic performance. Developing robust error quantification frameworks and systematic performance analysis methodologies is therefore of significant importance [8].

The Multiple Signal Classification (MUSIC) algorithm [9] marked a breakthrough in DOA estimation by achieving super-resolution performance. However, its reliance on exhaustive spectral peak searches results in high computational complexity, which limits practical applicability. To address this issue, the root-MUSIC algorithm [10] was introduced, significantly reducing computational burden. Nonetheless, both MUSIC and root-MUSIC operate in the complex domain, which can still pose efficiency challenges [11]. To further improve efficiency, real-valued subspace-based approaches such as Real-Valued MUSIC (RV-MUSIC) [12] and Real-Valued root-MUSIC (RV-root-MUSIC) [13, 14] have been proposed. While root-MUSIC performs well under high signal-to-noise ratio (SNR) and asymptotic conditions, its accuracy deteriorates considerably in low-SNR or limited-snapshot scenarios, i.e., non-asymptotic conditions. Although performance analyses for conventional complex-domain DOA estimation algorithms exist [15, 16], real-valued methods have not been thoroughly examined.

This paper addresses this gap by presenting a non-asymptotic performance analysis of RV-root-MUSIC. Theoretical error expressions are derived for both true and mirror roots, and their validity is verified through Monte Carlo simulations, which demonstrate close agreement between theoretical predictions and empirical results.

2. PRELIMINARIES

2.1. The model of the signal and arrays

Considering K far-field narrowband signals arriving on uniform linear arrays (ULA) with L elements, the ideal received array signal output at M snapshots can be expressed as:

$$\mathbf{X}(t) = \mathbf{A}(\theta)\mathbf{S}(t) \quad (1)$$

where $\mathbf{X}(t) \in \mathbb{C}^{L \times M}$ is the ideal received signal matrix, $\mathbf{A}(\theta) \in \mathbb{C}^{L \times K}$ is the array manifold matrix of ULA, con-

[†]Corresponding author: Qingping Wang

sisting of steering vectors as its columns, expressed as:

$$\mathbf{a}(\theta_k) = \left[1 \quad e^{-j\frac{2\pi d}{\lambda} \sin\theta_k} \quad \dots \quad e^{-j(L-1)\frac{2\pi d}{\lambda} \sin\theta_k} \right]^T \quad (2)$$

where d denotes the inter-element spacing, and λ is the signal wavelength. $\mathbf{S}(t) \in \mathbb{C}^{K \times M}$ is the source signal matrix.

When the perturbation $\Delta \mathbf{X}$ is taken into account, the above expression can be rewritten as:

$$\tilde{\mathbf{X}}(t) = \mathbf{X}(t) + \Delta \mathbf{X} = \mathbf{A}(\theta)\mathbf{S}(t) + \mathbf{N}(t) \quad (3)$$

where $\mathbf{N}(t) \in \mathbb{C}^{L \times M}$ is the additive noise matrix, typically modeled as complex circularly symmetric Gaussian.

In DOA estimation, the covariance matrix of received signals $\tilde{\mathbf{R}}_{xx}$ is commonly employed instead of the raw signal matrix $\tilde{\mathbf{X}}$ for analysis. This approach offers advantages such as accelerated computation through eigenvalue decomposition (EVD) and dimensionality reduction. $\tilde{\mathbf{R}}_{xx}$ is formulated as:

$$\tilde{\mathbf{R}}_{xx} = \frac{1}{M} \sum_{t=1}^M \tilde{\mathbf{X}}(t) \tilde{\mathbf{X}}^H(t) \quad (4)$$

2.2. Review about RV-root-MUSIC

The RV-root-MUSIC algorithm takes the real part of the covariance matrix, where the complex calculation of original root-MUSIC algorithm can be converted into the efficient real-valued one. Then EVD can be performed to extract the signal and noise subspace:

$$\tilde{\mathbf{R}}_{real} = \text{Re}(\tilde{\mathbf{R}}_{xx}) = \tilde{\mathbb{E}}_s \tilde{\Lambda}_s \tilde{\mathbb{E}}_s^T + \tilde{\mathbb{E}}_n \tilde{\Lambda}_n \tilde{\mathbb{E}}_n^T \quad (5)$$

where $\text{span}(\mathbb{E}_s)$ represents the real-valued eigenvectors spanning the signal subspace, with Λ_s denoting its associated diagonal eigenvalue matrix. The noise subspace components $\text{span}(\mathbb{E}_n)$ and Λ_n are defined analogously using real-valued quantities and $\tilde{\mathbf{R}}_{real} = \mathbf{R}_{real} + \Delta \mathbf{R}_{real}$, $\tilde{\mathbb{E}}_s = \mathbb{E}_s + \Delta \mathbb{E}_s$, $\tilde{\Lambda}_s = \Lambda_s + \Delta \Lambda_s$, $\tilde{\mathbb{E}}_n = \mathbb{E}_n + \Delta \mathbb{E}_n$, $\tilde{\Lambda}_n = \Lambda_n + \Delta \Lambda_n = \Delta \Lambda_n$.

Based on the defined noise subspace, the root-finding polynomial for RV-root-MUSIC can be constructed as:

$$f_{RV-root-MUSIC}(z) = \mathbf{p}^T(z^{-1}) \mathbb{E}_n \mathbb{E}_n^T \mathbf{p}(z) \quad (6)$$

where $\mathbf{p}(z)$ is defined as $[1, z, z^2, \dots, z^{M-1}]$, $z = e^{jw}$, and $w = \frac{2\pi d \sin\theta}{\lambda}$. Then based on the root-solving results, the DOA estimates can be calculated through:

$$\theta = \arcsin\left[\frac{\lambda}{2\pi d} \arg(z)\right] \quad (7)$$

As demonstrated in [13], RV-root-MUSIC suffers from the mirror roots, where the relationship $\theta_{mirror} = -\theta_{true}$ is satisfied. Thus the conventional beamforming (CBF) technique is typically employed to filter out the mirror roots as below:

$$\left| \mathbf{a}^H(\theta) \mathbf{R}_{xx} \mathbf{a}(\theta) \right|^2 \quad (8)$$

3. NON-ASYMPTOTIC PERFORMANCE ANALYSIS OF RV-ROOT-MUSIC

This paper makes a statistical characteristic analysis of real roots and mirror roots about RV-root-MUSIC under non-asymptotic conditions and also verifies the estimation accuracy with respect to the number of array elements.

The polynomial root-finding function of RV-root-MUSIC can be rewritten as:

$$f = AK(z)G(z) \quad (9)$$

where $K(z)$ denotes the roots related to the DOA roots:

$$K(z) = (1 - r_k z^{-1})(1 - r_k^* z)(1 - \frac{1}{r_k} z^{-1})(1 - \frac{1}{r_k^*} z) \quad (10)$$

while $G(z)$ represents other extraneous roots:

$$G(z) = \prod_{j=1, j \neq k}^{\lfloor \frac{L-1}{2} \rfloor} (1 - r_j \frac{1}{z})(1 - r_j^* z)(1 - \frac{1}{r_j} \frac{1}{z})(1 - \frac{1}{r_j^*} z) \quad (11)$$

As mentioned, RV-root-MUSIC can provide the mirror roots, therefore we can further divide $K(z)$ into the real root parts $K_{true}(z) = (1 - r_k z^{-1})(1 - r_k^* z)$ and the mirror root parts $K_{mirror}(z) = (1 - \frac{1}{r_k} z^{-1})(1 - \frac{1}{r_k^*} z)$:

$$K(z) = K_{true}(z)K_{mirror}(z) = K_t(z)K_m(z) \quad (12)$$

To derive the expression for the DOA estimation bias, we first define a logarithmic function $f(x) = \ln x$. Assume that $x = r_k$ is the root corresponding to the k -th DOA, and Δr_k denotes the error in estimating this root. The first-order Taylor expansion can be performed on $f(x)$ to obtain:

$$f(\tilde{r}_k) = \ln c + j\tilde{\omega}_k = \ln c + j\omega + f'(r_k)\Delta r_k \quad (13)$$

where $\tilde{r}_k = ce^{j\tilde{\omega}_k} = r_k + \Delta r_k$, $\tilde{\omega}_k = \omega_k + \Delta\omega_k$, and c is the amplitude perturbation caused by additive noise.

Using $f'(r_k) = 1/r_k$ and (13) can be simplified by canceling common terms, then take the imaginary part of both sides, we obtain:

$$\Delta\omega_k = \text{Im}\left(\frac{\Delta r_k}{r_k}\right) \quad (14)$$

Note that when $\Delta\theta_k \rightarrow 0$, the relationship $\Delta\omega_k = \frac{2\pi d}{\lambda} \cos\theta_k \Delta\theta_k$ is satisfied, we can further derive the bias expression of the final DOA estimation:

$$\Delta\theta_k = C_k \text{Im}\left(\frac{\Delta r_k}{r_k}\right) \quad (15)$$

where the scaling factor is $C_k = \frac{\lambda}{2\pi d \cos\theta_k}$. The derivation for mirror DOA follows the same procedure.

3.1. Deviation of the true DOAs

To derive the perturbation expression, $\text{Im}(\frac{\Delta r_k}{r_k})$ in (15) is necessary to be computed. The derivation can be decomposed into two steps:

step 1. Take the partial derivative with respect to the root z , and substitute $z = r_k$. Considering the perturbation of r , replace r_k with $\tilde{r} = r_k + \Delta(r_k)$ and only retain the first-order term to obtain the perturbation expression of r_k , as below:

$$\begin{aligned} \left. \frac{\partial f(z, \tilde{r})}{\partial z} \right|_{z=r_k} &= A[K_t(r_k)' [K_m(r_k)G(r_k)] \\ &\quad + K(r_k)[K_m(r_k)G(r_k)']] \Big|_{\tilde{r}=r_k+\Delta r_k} \quad (16) \\ &= A[K_t(r_k)' K_m(r_k)G(r_k)] \\ &\doteq 2jAr_k^* \text{Im}\left(\frac{\Delta r_k}{r_k}\right) K_m(r_k)G(r_k) \end{aligned}$$

step 2. As in **step 1**, but now consider the perturbation of \mathbb{E}_n , replace \mathbb{E}_n with $\tilde{\mathbb{E}}_n = \mathbb{E}_n + \Delta\mathbb{E}_n$ and retain only the first-order terms, we obtain:

$$\begin{aligned} \left. \frac{\partial f(z, \tilde{\mathbb{E}}_n)}{\partial z} \right|_{z=r_k} &= -r_k^2 \mathbf{p}^{(1)}(z^{-1})^T \tilde{\mathbb{E}}_n \tilde{\mathbb{E}}_n^T \mathbf{p}(z) \\ &\quad + \mathbf{p}(z^{-1})^T \tilde{\mathbb{E}}_n \tilde{\mathbb{E}}_n^T \mathbf{p}^{(1)}(z) \Big|_{z=r_k} \quad (17) \end{aligned}$$

where $p^{(1)}(z) = \frac{\partial p(z)}{\partial z}$. Substitute $\tilde{\mathbb{E}}_n = \mathbb{E}_n + \Delta\mathbb{E}_n$ and recognize the relation below:

$$\begin{cases} \mathbf{p}^T\left(\frac{1}{r_k}\right) = \mathbf{p}^T(r_k^*) = \mathbf{p}^H(r_k) \\ \mathbf{p}^{(1)}\left(\frac{1}{r_k}\right)^T = \mathbf{p}^{(1)}(r_k^*)^T = \mathbf{p}^{(1)}(r_k)^H \end{cases} \quad (18)$$

Given that $\mathbb{E}_n^T \mathbf{p}(r_k) = 0$ and the relation of (18), (17) can be simplified and we can further obtain the perturbation expression of \mathbb{E}_n as (19):

$$\left. \frac{\partial f(z, \tilde{\mathbb{E}}_n)}{\partial z} \right|_{z=r_k} \doteq 2jr_k^* \text{Im}[r_k \mathbf{p}^H(r_k) \Delta\mathbb{E}_n \mathbb{E}_n^T \mathbf{p}^{(1)}(r_k)] \quad (19)$$

Since the perturbation of r_k originates from the perturbation of \mathbb{E}_n , and both ultimately stem from noise, we can equate (16) and (19) to obtain:

$$\text{Im}\left(\frac{\Delta r_k}{r_k}\right) = \frac{\text{Im}[r_k \mathbf{p}^H(r_k) \Delta\mathbb{E}_n \mathbb{E}_n^T \mathbf{p}^{(1)}(r_k)]}{AK_m(r_k)G(r_k)} \quad (20)$$

Substituting to the derived equation (15) above yields:

$$\Delta\theta_k = \frac{\lambda}{2\pi d \cos\theta_k} \frac{\text{Im}[r_k \mathbf{p}^H(r_k) \Delta\mathbb{E}_n \mathbb{E}_n^T \mathbf{p}^{(1)}(r_k)]}{AK_m(r_k)G(r_k)} \quad (21)$$

3.2. Deviation of the mirror DOAs

Since the relationship $r_{\varphi_k} = r_{\theta_k}^*$ is satisfied for the mirror roots $\varphi_k = -\theta_k$, their analysis can be directly obtained by

substituting $z = r_k^*$ into the derivations from the previous section.

Following the same procedure as in the previous **step 1**, we can derive the perturbation expression of r_k^* :

$$\begin{aligned} \left. \frac{\partial f(z, \tilde{r})}{\partial z} \right|_{z=r_k^*} &= A[K_m(r_k^*)' [K_t(r_k^*)G(r_k^*)] \\ &\quad + K_m(r_k^*)[K_t(r_k^*)G(r_k^*)']] \Big|_{\tilde{r}=r_k^*+\Delta(r_k^*)} \quad (22) \\ &= A[K_m(r_k^*)' K_t(r_k^*)G(r_k^*)] \Big|_{\tilde{r}=r_k^*+\Delta(r_k^*)} \\ &\doteq 2jAr_k^* \text{Im}\left(\frac{\Delta r_k^*}{r_k^*}\right) K_t(r_k^*)G(r_k^*) \end{aligned}$$

and the perturbation expression of \mathbb{E}_n as **step 2**:

$$\begin{aligned} \left. \frac{\partial f(z, \tilde{\mathbb{E}}_n)}{\partial z} \right|_{z=r_k^*} &= -r_k^2 \mathbf{p}^{(1)}(z^{-1})^T \tilde{\mathbb{E}}_n \tilde{\mathbb{E}}_n^T \mathbf{p}(z) \\ &\quad + \mathbf{p}(z^{-1})^T \tilde{\mathbb{E}}_n \tilde{\mathbb{E}}_n^T \mathbf{p}^{(1)}(z) \Big|_{z=r_k^*} \quad (23) \end{aligned}$$

where $p^{(1)}(z) = \frac{\partial p(z)}{\partial z}$. Substitute $\tilde{\mathbb{E}}_n = \mathbb{E}_n + \Delta\mathbb{E}_n$ and recognize the relation below:

$$\begin{cases} \mathbf{p}^T\left(\frac{1}{r_k^*}\right) = \mathbf{p}^T(r_k) = \mathbf{p}^H(r_k^*) \\ \mathbf{p}^{(1)}\left(\frac{1}{r_k^*}\right)^T = \mathbf{p}^{(1)}(r_k)^T = \mathbf{p}^{(1)}(r_k^*)^H \end{cases} \quad (24)$$

Given that $\mathbb{E}_n^T \mathbf{p}(r_k^*) = 0$ and the relation of (24), (23) can be simplified and we can further obtain the perturbation expression of \mathbb{E}_n as (25):

$$\left. \frac{\partial f(z, \tilde{\mathbb{E}}_n)}{\partial z} \right|_{z=r_k^*} \doteq 2jr_k^* \text{Im}[r_k^* \mathbf{p}^H(r_k^*) \Delta\mathbb{E}_n \mathbb{E}_n^T \mathbf{p}^{(1)}(r_k^*)] \quad (25)$$

By the equivalence of perturbations, we can get:

$$\text{Im}\left(\frac{\Delta r_k^*}{r_k^*}\right) = \frac{\text{Im}[r_k^* \mathbf{p}^H(r_k^*) \Delta\mathbb{E}_n \mathbb{E}_n^T \mathbf{p}^{(1)}(r_k^*)]}{AK_t(r_k^*)G(r_k^*)} \quad (26)$$

and further obtain:

$$\Delta\varphi_k = \frac{\lambda}{2\pi d \cos\varphi_k} \frac{\text{Im}[r_k^* \mathbf{p}^H(r_k^*) \Delta\mathbb{E}_n \mathbb{E}_n^T \mathbf{p}^{(1)}(r_k^*)]}{AK_t(r_k^*)G(r_k^*)} \quad (27)$$

It should be noted that Δr_k^* represents the perturbation at $z = r_k^*$, while $(\Delta r_k)^*$ denotes the complex conjugate of the perturbation at $z = r_k$. These are fundamentally different quantities, as: $\Delta r_k^* \neq (\Delta r_k)^*$, $(\Delta r_k^*)^* \neq \Delta r_k$. This reflects how the function's perturbation behavior varies at different evaluation points.

3.3. Deviation of the Noise subspace

Both (21) and (27) reveal that biases $\Delta\theta_k$ and $\Delta\varphi_k$ originate from perturbations in the noise subspace. The noise subspace perturbation is derived as follow:

We define a new signal model $\mathbf{X}_v = [\mathbf{X} \ \mathbf{X}^*]$, where the following properties are satisfied after considering the noise:

$$\tilde{\mathbf{X}}_v \tilde{\mathbf{X}}_v^H = 2\text{Re}(\tilde{\mathbf{X}} \tilde{\mathbf{X}}^H) = 2M\text{Re}(\tilde{\mathbf{R}}_{xx}) \quad (28)$$

where $\tilde{\mathbf{X}}_v = \mathbf{X}_v + \Delta\mathbf{X}_v$, $\Delta\mathbf{X}_v = [\Delta\mathbf{X} \ \Delta\mathbf{X}^*]$. Then Singular Value Decomposition (SVD) of $\tilde{\mathbf{X}}_v$ and EVD of $\tilde{\mathbf{R}}_{real}$ yield the following results:

$$\begin{cases} \tilde{\mathbf{X}}_v = \tilde{\mathbf{U}}_s \tilde{\mathbf{W}}_s \tilde{\mathbf{V}}_s^H + \tilde{\mathbf{U}}_n \tilde{\mathbf{W}}_n \tilde{\mathbf{V}}_n^H \\ \tilde{\mathbf{R}}_{real} = \tilde{\mathbb{E}}_s \tilde{\Lambda}_s \tilde{\mathbb{E}}_s^T + \tilde{\mathbb{E}}_n \tilde{\Lambda}_n \tilde{\mathbb{E}}_n^T \end{cases} \quad (29)$$

where $\tilde{\mathbf{U}}_s = \mathbf{U}_s + \Delta\mathbf{U}_s$, $\tilde{\mathbf{W}}_s = \mathbf{W}_s + \Delta\mathbf{W}_s$, $\tilde{\mathbf{V}}_s = \mathbf{V}_s + \Delta\mathbf{V}_s$, $\tilde{\mathbf{U}}_n = \mathbf{U}_n + \Delta\mathbf{U}_n$, $\tilde{\mathbf{W}}_n = \mathbf{W}_n + \Delta\mathbf{W}_n$, $\tilde{\mathbf{V}}_n = \mathbf{V}_n + \Delta\mathbf{V}_n$.

Substituting (29) into (28) can yield:

$$\tilde{\mathbf{U}}_s \tilde{\mathbf{W}}_s^2 \tilde{\mathbf{U}}_s^H + \tilde{\mathbf{U}}_n \tilde{\mathbf{W}}_n \tilde{\mathbf{W}}_n^T \tilde{\mathbf{U}}_n^H = 2M(\tilde{\mathbb{E}}_s \tilde{\Lambda}_s \tilde{\mathbb{E}}_s^T + \tilde{\mathbb{E}}_n \tilde{\Lambda}_n \tilde{\mathbb{E}}_n^T) \quad (30)$$

Observing (30), we can obtain following relationships:

$$\tilde{\mathbf{U}}_s = \tilde{\mathbb{E}}_s, \tilde{\mathbf{U}}_n = \tilde{\mathbb{E}}_n, \tilde{\mathbf{W}}_s^2 = 2M\tilde{\Lambda}_s, \tilde{\mathbf{W}}_n \tilde{\mathbf{W}}_n^T = 2M\tilde{\Lambda}_n \quad (31)$$

As derived in [15], for ULA, the perturbation of the noise subspace in the singular value domain of the received signal matrix $\tilde{\mathbf{X}}$ can be expressed as:

$$\Delta\mathbf{U}_o = -\mathbf{U}_s \mathbf{W}_s^{-1} \mathbf{V}_s^H \Delta\mathbf{X}^H \mathbf{U}_o \quad (32)$$

Based on (32) and the equivalent noise subspace characterization, we derive the noise subspace perturbation for RV-root-MUSIC as:

$$\Delta\mathbb{E}_n = \Delta\mathbf{U}_n = -\mathbf{U}_s \mathbf{W}_s^{-1} \mathbf{V}_s^H \Delta\mathbf{X}_v^H \mathbf{U}_n \quad (33)$$

where $\Delta\mathbf{X}_v = \mathbf{N}_v = [\Delta\mathbf{X} \ \Delta\mathbf{X}^*] = [\mathbf{N} \ \mathbf{N}^*]$.

3.4. Root Pairs of RV-root-MUSIC in even array elements

Theorem: For ULA with even elements, at least one root pair degenerates onto the real axis, corresponding to spurious DOA at 0° or 180° that align with the ULA axis. (see Fig. 1)

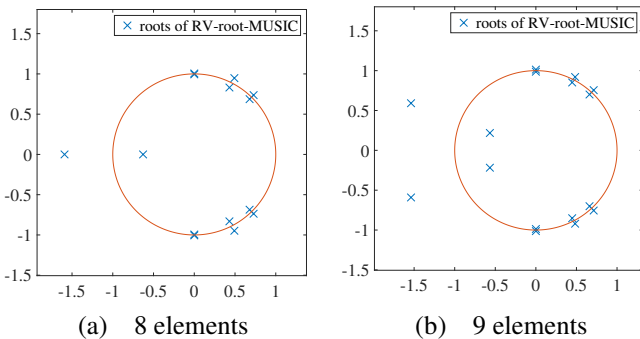


Fig. 1: Roots of RV-root-MUSIC in varying array elements

Proof: An odd-degree polynomial can be expressed as:

$$y = a_n x^n + a_{n-1} x^{n-1} + \dots + a_1 x + a_0 \quad (34)$$

where $a_n \neq 0$ and n is a positive odd integer. Dividing both sides by x^n and taking the limit as $x \rightarrow \infty$ yields:

$$\lim_{x \rightarrow \infty} \frac{y}{x^n} = \lim_{x \rightarrow \infty} a_n + \frac{a_{n-1}}{x} + \dots = a_n \quad (35)$$

Furthermore, since n is odd, we have:

$$\lim_{x \rightarrow +\infty} x^n = +\infty \quad \lim_{x \rightarrow -\infty} x^n = -\infty \quad (36)$$

By the continuity of y and its behavior at infinity, it can be obtained that there exist points in \Re where y changes sign. The Intermediate Value Theorem guarantees the existence of at least one real root satisfying $y = 0$. Extending to the complex domain, for even-numbered arrays, (6) will transform into an odd-degree polynomial, and there must exist a pair of reciprocal roots on the real axis. **Proof** completed.

Therefore, for the framework proposed in (11), we derive a correction factor $R(a)$ for even-numbered arrays as follows:

$$R(a) = a^2 - 2a\text{Re}(r_k) + 1 = a^2 - 2a\text{Re}(r_k^*) + 1 \quad (37)$$

where a is the real root previously discussed. To get more precise perturbation value, just multiply (21) and (27) by $\frac{1}{R(a)}$.

4. STATISTICAL PROPERTIES OF TRUE AND MIRROR DOA PERTURBATIONS

Substituting (33) into (21) and (27), identical forms can be observed. To simplify the performance analysis model, the general perturbation expression Δ_k can be expressed as:

$$\Delta_k = -\frac{\text{Im}(\beta_k^H \mathbf{N}_v^H \alpha_k)}{\gamma_k} \quad (38)$$

where the parameters $\alpha_k, \beta_k, \gamma_k$ are specified in Table 1.

Given that bias has zero mean and each element of the random variable $\Delta\mathbf{X}_v$ has variance $\sigma_n^2/2$ for both real and imaginary components, the MSE of bias is as follows:

$$E_{\mathbf{N}_v}(\Delta_k)^2 = \frac{E_{\mathbf{N}_v}[|\beta_k^H \mathbf{N}_v^H \alpha_k|^2]}{2\gamma_k^2} = \frac{\|\alpha_k\|^2 \|\beta_k\|^2 \sigma_n^2}{2\gamma_k^2} \quad (39)$$

Table 1: The parameters in the general expression

	α_k	β_k	γ_k
$\Delta\theta_k$	$\mathbb{E}_n \mathbb{E}_n^T \mathbf{p}^{(1)}(r_k) C_k r_k$	$\mathbf{V}_s \mathbf{W}_s^{-1} \mathbf{U}_s^H \mathbf{p}(r_k)$	$AK_m(r_k)G(r_k)$
$\Delta\varphi_k$	$\mathbb{E}_n \mathbb{E}_n^T \mathbf{p}^{(1)}(r_k^*) C_k r_k^*$	$\mathbf{V}_s \mathbf{W}_s^{-1} \mathbf{U}_s^H \mathbf{p}(r_k^*)$	$AK_t(r_k^*)G(r_k^*)$

5. SIMULATION EXPERIMENTS AND RESULTS

5.1. Experimental Setup and Results

To analyze the statistical impact of noise on DOA estimation, we conduct Monte Carlo simulations to examine the variation of estimation bias under zero-mean additive white Gaussian noise conditions.

A 9-element ULA with $d = \lambda/2$ is used in the simulation, with two uncorrelated sources at 30° and 50° . DOA estimation RMSEs for the source at 30° from 1000 Monte Carlo trials are investigated under 2 conditions:

condition 1: Varying the SNR from 0dB to 20dB in 2dB steps with 200 snapshots, and the result is shown in Fig. 2.

condition 2: Varying the snapshots 2^n , where n varies from 5 to 12 in 1 step at 10dB SNR, with the result shown in Fig. 3.

From Fig. 2, the RMSE decreases as the SNR increases, and the simulation performance aligns with the theoretical performance more and more closely.

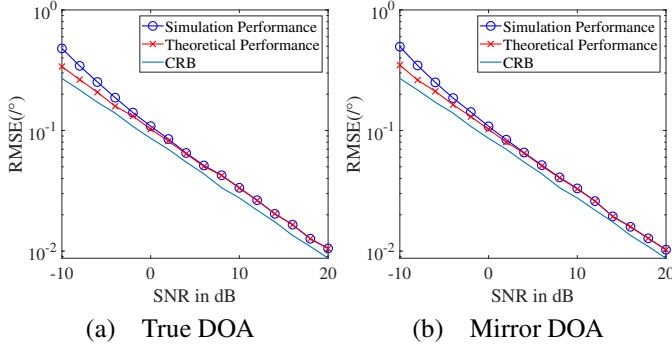


Fig. 2: The trend of estimation RMSE in SNR variation

From Fig. 3, the RMSE decreases with increasing snapshot number, though the rate of improvement diminishes progressively. Beyond a certain threshold, further increases in computational complexity and processing time yield marginal performance gains. Consequently, selecting an appropriate snapshot count that balances resolution accuracy and computational efficiency is critical.

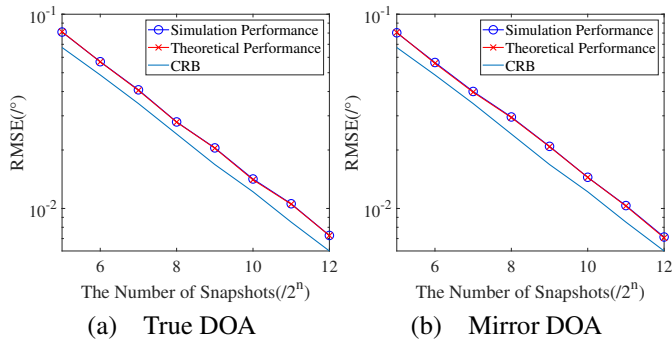


Fig. 3: The trend of estimation RMSE in Snapshots variation

From Fig. 2 and Fig. 3, it can be seen that the simulation performance closely aligns with the theoretical performance.

5.2. Experimental Conclusion

From the above experiments, it can be seen that the trends of the simulation performance and theoretical performance varying with the SNR and the number of snapshots are basically consistent. The theoretical performance provides a tighter theoretical lower bound for RV-root-MUSIC.

6. CONCLUSION

This paper presented a non-asymptotic performance analysis framework for the RV-root-MUSIC algorithm. Unlike prior works that mainly focus on asymptotic or complex-domain analyses, the proposed framework systematically characterizes the perturbation behavior of the noise subspace, true roots, and mirror roots in the real-valued setting. A statistical model was developed, and generalized perturbation expressions were derived, providing a unified formulation for both true and mirror DOA deviations. Monte Carlo simulations confirmed the theoretical predictions, demonstrating close alignment with the analytical results.

Beyond the theoretical contributions, this work offers several practical insights:

- The analysis establishes a tighter theoretical performance bound for RV-root-MUSIC in finite-snapshot and low-SNR regimes, which are highly relevant to real-world radar, communications, and sensing systems.
- The investigation of array element parity revealed that even-element ULAs suffer from root degeneracy on the real axis, leading to spurious DOAs at broadside directions. The proposed correction factor and the recommendation to employ odd-element arrays provide a design guideline for practitioners to enhance algorithm robustness.
- The derived perturbation expressions enable parameter optimization (e.g., array size, number of snapshots, and SNR trade-offs), offering practical value for system design under constrained computational resources.

Overall, this paper advances the theoretical understanding of RV-root-MUSIC under non-asymptotic conditions and bridges the gap between abstract perturbation theory and practical DOA estimation design. Future work will extend the framework to correlated sources, arbitrary array geometries, and adaptive mirror-root suppression techniques, further enhancing its applicability in modern sensing and communication platforms.

7. FUNDING ACKNOWLEDGEMENTS

The work of X. T. Meng is supported by the Shandong Provincial Natural Science Foundation (No.ZR2024QF068). The work of F. Gini and M. Greco has been partially supported by the Italian Ministry of Education and Research (MUR) in the framework of the FoReLab project (Departments of Excellence).

8. REFERENCES

- [1] H. Krim and M. Viberg, "Two decades of array signal processing research: the parametric approach," *IEEE Signal Processing Magazine*, vol. 13, no. 4, pp. 67–94, 1996.
- [2] A. Khabbazibasmenj, A. Hassaniien, S. A. Vorobyov, and M. W. Morency, "Efficient transmit beamspace design for search-free based doa estimation in mimo radar," *IEEE Transactions on Signal Processing*, vol. 62, no. 6, pp. 1490–1500, 2014.
- [3] R. Pec, T. H. Hong, and Y. S. Cho, "Cell searching and doa estimation for a mobile relay station in a multipath environment," *Journal of Communications and Networks*, vol. 15, no. 2, pp. 191–197, 2013.
- [4] J. Zhu, H. Veeraraghavan, J. Jiang, J. H. Oh, L. Norton, J. O. Deasy, and A. Tannenbaum, "Wasserstein hog: Local directionality extraction via optimal transport," *IEEE Transactions on Medical Imaging*, vol. 43, no. 3, pp. 916–927, 2024.
- [5] H. L. Van Trees, *Optimum Array Processing: Part IV of Detection, Estimation, and Modulation Theory*. Hoboken, NJ, USA: Wiley, 2002.
- [6] H. Zhang, W. Liu, Q. Zhang, and B. Liu, "Joint customer assignment, power allocation, and subchannel allocation in a uav-based joint radar and communication network," *IEEE Internet of Things Journal*, vol. PP, pp. 1–1, 09 2024.
- [7] H. Zhang, W. Liu, Q. Zhang, L. Zhang, B. Liu, and H.-X. Xu, "Joint power, bandwidth, and subchannel allocation in a uav-assisted dfrc network," *IEEE Internet of Things Journal*, vol. PP, pp. 1–1, 05 2025.
- [8] J. Zhang, F. Kang, Z. Liu, Z. Qu, M. Xu, S. Zha, and P. Liu, "Design of ultrawideband energy-selective surface based on triple-layer structure and semiconductor for HIRF prevention," *IEEE Transactions on Antennas and Propagation*, vol. 73, pp. 9619–9624, Nov 2025.
- [9] R. Schmidt, "Multiple emitter location and signal parameter estimation," *IEEE Transactions on Antennas and Propagation*, vol. 34, no. 3, pp. 276–280, 1986.
- [10] A. Barabell, "Improving the resolution performance of eigenstructure-based direction-finding algorithms," in *ICASSP '83. IEEE International Conference on Acoustics, Speech, and Signal Processing*, vol. 8, pp. 336–339, 1983.
- [11] F. Yan, M. Jin, H. Zhou, J. Wang, and S. Liu, "Low-degree root-music algorithm for fast doa estimation based on variable substitution technique," *Science China(Information Sciences)*, vol. v.63, no. 05, pp. 218–220, 2020.
- [12] F.-G. Yan, M. Jin, S. Liu, and X.-L. Qiao, "Real-valued music for efficient direction estimation with arbitrary array geometries," *IEEE Transactions on Signal Processing*, vol. 62, no. 6, pp. 1548–1560, 2014.
- [13] F.-G. Yan, Y. Shen, and M. Jin, "Fast doa estimation based on a split subspace decomposition on the array covariance matrix," *Signal Processing*, vol. 115, pp. 1–8, 2015.
- [14] F.-G. Yan, L. Shuai, J. Wang, J. Shi, and M. Jin, "Real-valued root-music for doa estimation with reduced-dimension evd/svd computation," *Signal Process.*, vol. 152, p. 1–12, Nov. 2018.
- [15] F. Li, H. Liu, and R. Vaccaro, "Performance analysis for doa estimation algorithms: unification, simplification, and observations," *IEEE Transactions on Aerospace and Electronic Systems*, vol. 29, no. 4, pp. 1170–1184, 1993.
- [16] B. Rao and K. Hari, "Performance analysis of root-music," *IEEE Transactions on Acoustics, Speech, and Signal Processing*, vol. 37, no. 12, pp. 1939–1949, 1989.